Diffusion versus Cocrystallization of Very Long Polymer Chains at Interfaces: Experimental Study of Sintering of UHMWPE Nascent Powder

ARTICLE *in* MACROMOLECULES · DECEMBER 2013

Impact Factor: 5.8 · DOI: 10.1021/ma402012f

6 AUTHORS, INCLUDING:

Tiana Deplancke
Grenoble Institute of Technology
9 PUBLICATIONS **6** CITATIONS

SEE PROFILE

Olivier Lame
Institut National des Sciences Appliquées de L…
50 PUBLICATIONS **514** CITATIONS

SEE PROFILE

Francois Rousset
Institut National des Sciences Appliquées de L…
30 PUBLICATIONS **78** CITATIONS

SEE PROFILE

Macromolecules

Article

pubs.acs.org/Macromolecules

Diffusion versus Cocrystallization of Very Long Polymer Chains at Interfaces: Experimental Study of Sintering of UHMWPE Nascent Powder

T. Deplancke,[†] O. Lame,*[,†] F. Rousset,[‡,§] I. Aguili,[†] R. Seguela,[†] and G. Vigier[†]

[†]MATEIS, CNRS INSA Lyon UMR5510, Bat. Blaise Pascal, 69621 Villeurbanne, France

[‡]Univ-Lyon, CNRS INSA Lyon UMR5008, CETHIL, Bat. Sadi Carnot, 69621 Villeurbanne, France

[§]Univ-Lyon1, 69622 Villeurbanne, France

Supporting Information

ABSTRACT: Ultrahigh-molecular-weight polyethylene (UHMWPE) has been processed by means of sintering of a nascent powder. Particular attention was paid to the precompaction of the powder just below the melting point (T_m) under vacuum. The particle welding was subsequently carried out under pressure at various temperatures above T_m for various durations. Tensile drawing experiments performed on sintered samples either at room temperature or above T_m were specifically aimed at discriminating the role of chain interdiffusion through the particle interfaces from that of cocrystallization in the mechanism of particle welding. It turned out that efficient welding occurred within a very short time. One of the novel results of the work is the much weaker influence of sintering time as compared with temperature, giving evidence that chain interdiffusion is not governed by a reptation process. The entropy-driven melting explosion over distances much larger than the chain length between entanglements is suggested to be the main mechanism of the fast chain re-entanglement and particle welding in the present case of a nascent powder consisting of nonequilibrium chain-disentangled crystals. Another major aspect of this study is the demonstration of the huge cocrystallization efficiency in the interface consolidation in the solid state that significantly hides the kinetics of chain intertwining occurring in the melt.

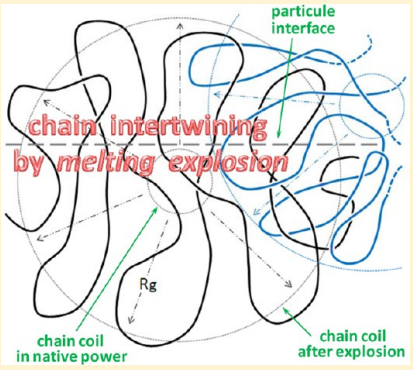

INTRODUCTION

Ultrahigh-molecular-weight polyethylene (UHMWPE) is a high performance polymer that is used in the domain of joint arthroplasty and number of applications demanding toughness, wear resistance, and low friction. However, conventional processing of UHMWPE is nearly impossible due to its very high viscosity. As a consequence, processes inspired from powder metallurgy such as sintering have been developed. Understanding the kinetic aspects of the process should contribute to progress in the knowledge of the diffusion mechanisms of extremely long molecules and would greatly help improving the mechanical properties and durability of the sintered parts, particularly in the case of joint prosthesis applications that is an acute scientific challenge.

The sintering of polymer powders involves healing of the particle interfaces, a process that is often described in two stages.[1] The first one is the densification of the powder associated with the wetting of the grains. It can be efficiently performed below the melting temperature in the case of semicrystalline polymers.[2] The second stage is the diffusion of the chains across interfaces leading to the consolidation of the interfaces by chain re-entanglement.[3] At this stage, the polymer is necessarily melted and two parameters play a major role, namely time and temperature. In polymer melts, diffusion mechanisms are generally described using the reptation theory.[4,5] Reptation proved to be the relevant mechanism of polymer chain diffusion that allowed interpreting the experimental results concerning the consolidation of polymer interfaces in the case of crack healing or welding.[6−9]

Two main features of the kinetics of reptation have to be noticed. First, it strongly depends of the molecular mass of the polymer which is responsible for the huge viscosity of UHMWPE. Second, reptation kinetics exhibits an equivalent dependence on time and temperature in contrast to Arrhenian phenomena. It can be easily shown that the interpenetration distance of a chain during healing or welding process (i.e., the distance covered by a molecule across the initial interface) varies as $(Tt)^{\gamma}$, where T and t are respectively the temperature and the time. This relationship will be details further in the Discussion section. The re-entanglement rate in the interfacial region is then expected to be proportional to $(Tt)^{\gamma}$ as well. Depending on time scale, the γ value can be either 1/2 or 1/4 as given in Wool[1] and Bousmina.[3] The mechanical properties of welded or healed polymer interfaces are generally supposed

Received: September 29, 2013
Revised: December 6, 2013
Published: December 18, 2013

to mainly depend on the re-entanglement density in the interfacial region.[6−9] Therefore, mechanical properties of sintered materials should evolve similarly with time and temperature of sintering.

In addition, for semicrystalline polymers, it is also possible to promote the interface consolidation by cocrystallization of the chains after interdiffusion.[10−13] Cocrystallization consists in the growth of new crystallites across the interface binding the initial powder particles. Recent studies on UHMWPE have even shown that very short diffusion time is sufficient to give a rather high ductility to welded interfaces[14] and sintered powders as well.[15−17] It is quite clear that the final mechanical properties of a sintered semicrystalline polymer such as UHMPWE are the result of both the reconstitution of an entanglement network and the buildup of a crystalline network in the interfacial regions of the sintered powder.

In this paper, we take benefit from the exceptional temperature extent of the rubbery plateau of UHMWPE beyond its melting point to perform tensile tests in the molten state. In such circumstances, crystallites are eliminated so that UHMWPE behaves like a rubber. Its mechanical properties are then essentially governed by the entanglement network that should strongly depend on the sintering conditions. First, we address the issue of the time/temperature equivalence predicted by the reptation theory by performing a series of tensile tests above the melting point for different sintering conditions. Second, by comparing tensile tests at room temperature and tensile tests above the melting point, we address the question of the respective contributions of the entanglement network and the crystalline network and their evolution as a function of the sintering conditions.

EXPERIMENTAL SECTION

Material: Structural and Physical Characterization. The UHMWPE under investigation is a nascent reactor powder produced by Ticona (Oberhausen, Germany) under trade name GUR4113. The molecular mass deduced from viscosity measurements is 3900 kg/mol. The average grain size is 150 μm, and the statistical distribution extends from 50 to 500 μm, as measured by the laser scattering technique. The crystallinity ratio was measured by DSC using a PerkinElmer Pyris apparatus at a heating rate of 10 °C/min. The temperature and heat flow scales were calibrated using high-purity indium.

Density measurements were performed using the buoyancy method based on Archimedes' principle. Density data were compared with those computed from the DSC crystal ratio in order to estimate the remaining porosity of the sintered materials taking ρ_a = 0.855 g/cm^3 and ρ_c = 1.000 g/cm^3 for the densities of the amorphous and the crystalline phases, respectively.

Small-angle X-ray scattering (SAXS) is a powerful tool for detection of nanoscopic porosities due to the high electron density contrast between matter and cavities. Measurements were performed on a laboratory bench using the Cu Kα radiation of a Rigaku rotating anode equipped with point focusing multilayer optics from Xenocs. The 2D frames were recorded on a CCD camera from Princeton Instruments.[18]

Thermogravimetric measurements were carried out on a Netzsch apparatus model TG209F3 in order to control thermodegradation under a nitrogen atmosphere. Samples about 10 mg in weight were heated at a scanning rate of 5 °C/min up to 600 °C for complete degradation.

Morphological investigations were performed by scanning electron microscopy (SEM) using a Carl Zeiss SUPRA 55VP apparatus operated at 1 kV. No metal coating was applied to the samples prior to the SEM observations.

Dynamic mechanical analysis (DMA) was performed using a homemade torsion pendulum[19] at a frequency of 1 Hz, with sample dimensions 10 × 3 × 1 mm. Data were recorded at a heating rate of 1 °C/min over the temperature range 25−350 °C for computing the shear modulus G'.

Sintering Protocol. Sintering classically operates via two stages. In a first stage, the precompaction or densification of the powder aims at achieving the wetting of the surfaces of the powder grains. As already pointed out by several authors,[1,8,12−14] this stage is crucial for the efficiency of welding or healing of polymer interfaces. In a second stage, consolidation of the interfaces takes place via chain diffusion and chain re-entanglement. This second stage is the one which controls the interface consolidation, i.e., the completion of sintering.

Sintering of the present UHMWPE nascent powder was performed in an Instron compressive testing machine equipped with a Servantin oven. For a better control of the molecular mechanisms of sintering, the two main stages of the process were carried out separately as described in Figure 1. In a first stage, densification (Figure 1a) was

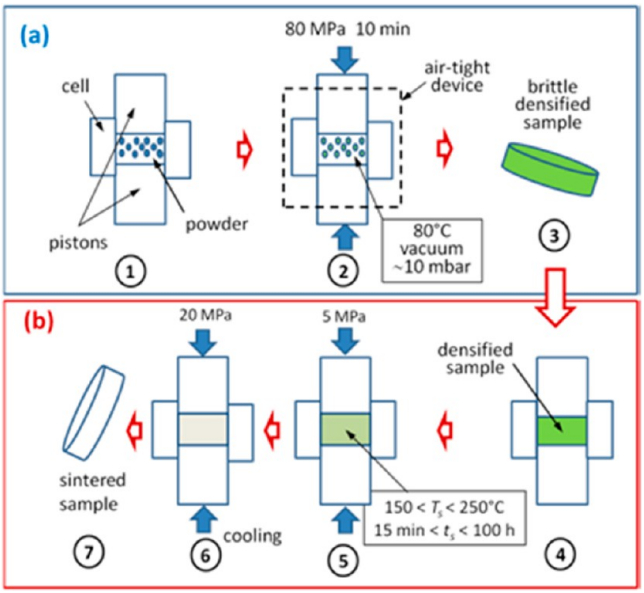

Figure 1. Sketch of sintering protocol: (a) first stage, densification; (b) second stage, consolidation.

performed in a stainless steel cell equipped with an airtight vacuum device to rule out air porosities. This apparatus allowed to simultaneously apply compressive stress and vacuum. The sample powder was introduced into the cell between the two pistons (step 1). It was then heated up at 80 °C for 10 min under compressive stress of 80 MPa and vacuum of about 10 mbar (step 2). The fact of maintaining the temperature below the temperature of fusion, T_f, enabled ensuring negligible chain diffusion across the particle interfaces. The densification conditions were empirically optimized and validated by density measurements. Occasionally, samples were extracted from the cell (step 3) for controlling perfect densification by comparing the measured density to that computed from the DSC crystallinity. The samples were yet very brittle after this first stage.

The second stage of the process (Figure 1b) is the consolidation of interfaces by chain diffusion. Using the same compaction cell without its vacuum device (step 4), the densified sample was heated up beyond the melting point under a constant pressure of 5 MPa during variable lapses of time (step 5). The pressure cycle was the same for all samples, whereas the sintering temperature and time varied in the ranges 150 °C < T_s < 250 °C and 15 min < t_s < 100 h, respectively. Hereafter, the sample was cooled down to room temperature under 20 MPa (step 6) in order to prevent shrinkage cavities. The sintered sample was finally ejected from the cell (step 7).

dx.doi.org/10.1021/ma402012f | Macromolecules 2014, 47, 197−207

The temperatures and durations of sintering used in this study are summarized in Table 1. It was not possible to perform sintering

Table 1. Temperature (T_s) and Time (t_s) of Sintering Used in the Present Work[a]

t_s(h) \ T_s(°C)	150	170	180	190	200	220	250
0.25	■				■		
1	■				■		
2	■	■	■	■	■	■	■
5	■				■		
20	■				■		
100					■		

[a]The tested conditions are indicated by the gray cells.

experiments with t_s < 15 min due to the minimum time necessary for heating the sintering device. Absence of degradation during sintering in the range 150 °C < T_s < 250 °C was checked by thermogravimetric analysis: the present UHMWPE material displayed not any degradation before 350 °C under a nitrogen atmosphere. No measurable degradation occurred as well when holding the sample for 20 h at 200 °C.

Disks 2 mm in thickness and 25 mm in diameter were obtained. Dumbbell-shaped specimens having 22 mm in gauge length and 5 mm in width were punched out with a die from the disks for tensile tests.

Mechanical Characterization of Sintered Materials. Borrowing from Xue et al.,[14] tensile tests have been carried out both below and above the melting point, namely in the solid state at room temperature, RT, and in the rubbery state at 150 °C. The main interest of this dual mechanical approach is to discriminate the two contributions to the particle welding, i.e., chain re-entanglement and cocrystallization. All tensile tests were performed using a tensile machine MTS 1/ME equipped with an oven MTS CE412. The tensile machine was fitted with two kinds of load cells, one having a 5 kN range for tensile tests at RT and the other one having a 100 N range for tensile tests at 150 °C.

For the tensile tests at RT the cross-head speed was 2 mm/min, so that the initial strain rate was 3.5×10^{-3} s^{-1}. For the tensile tests at 150 °C, the cross-head speed was 6 mm/min; thus, the initial strain rate was 10^{-2} s^{-1}. The sample temperature was checked by means of a thermocouple glued to the head of the tensile specimen. The temperature gradient over the sample length did not exceed 3 °C. The time necessary for heating the tensile grips and sample was 15 min, the holding time of the sample above T_f being about 5 min. These conditions were fairly repeatable, so that the results from different sintering treatments can be compared. Tensile tests were repeated four times for every sintering conditions.

Considering the nearly homogeneous deformation of all samples irrespective of sintering and drawing conditions, the true strain was computed as $\varepsilon = \ln(L/L_0)$, where L_0 is the initial sample gauge length and L its length under straining. The true stress was defined as $\sigma = F\lambda/S_0$, where F is the tensile force, $\lambda = L/L_0$ is the draw ratio, and S_0 is the initial sample cross section. This computation assumes isovolumic strain, neglecting Poisson's effect and cavitation. The elastic modulus was computed from a linear regression on the experimental data in the strain range 0.01 < ε < 0.03 to avoid experimental errors from both strain onset determination and viscoplastic deformation.

In addition to tensile measurements, the entropic strain recovery after tensile drawing up to rupture in the rubbery state at 150 °C was determined according to the relation

$$R = \frac{L_s - L_r}{L_s - L_0} \quad (1)$$

where L_s is the sample length at rupture, L_0 is the initial sample gauge length, and L_r is the sample length after recovery.

RESULTS AND DATA ANALYSIS

Structural and Physical Properties of the Material. The DSC curves displayed on of Figure 2 show the melting

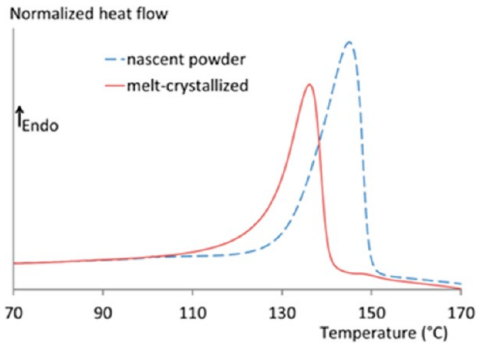

Figure 2. DSC curves of the nascent powder and the melt-crystallized material.

endotherm of the nascent powder and that of the recrystallized material following the first heating run. The much higher crystallinity and melting point of the present powder are characteristic of UHMWPE nascent reactor powders.[20−27] The surprisingly high melting temperature has been assigned to nonequilibrium chain conformations, but the actual origin is not clearly understood: the presence of chain-extended crystals[20,21] as well as constrained chain-folded crystals[25,26] has been proposed.

Nonetheless, one of the nonambiguous characteristics of the chain topology of UHMWPE nascent powders is the low level of chain entanglement compared to their melt-crystallized parents. Indeed, the in-situ crystallization of individual chains during slurry catalytic polymerization prevents entanglement with the neighbor chains.[21−23] This applies to the UHMWPE nascent powder under consideration in this study. However, the phenomenon is more or less pronounced depending on the polymerization temperature that is unknown in the present case. Thereby, we may assume that the present UHMWPE nascent powder is actually in a nonequilibrium and disentangled state, without quantitative assessment yet.

This material was chosen because of its very high viscosity in the melt that results in an extremely broad rubbery plateau as can be seen on the shear modulus versus temperature plot displayed in Figure 3. This exceptional property enables to perform tensile drawing experiments below as well as above the melting point. This enables to split studies of the two main

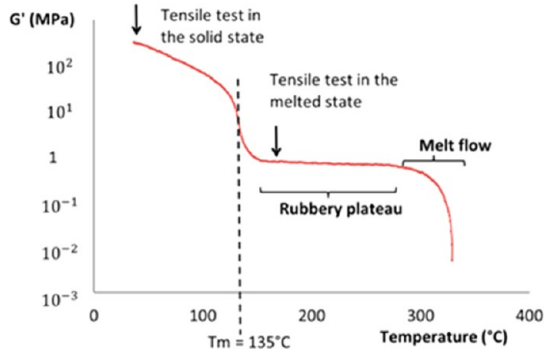

Figure 3. Elastic shear modulus of UHMWPE versus temperature (f = 1 Hz).

dx.doi.org/10.1021/ma402012f | Macromolecules 2014, 47, 197−207

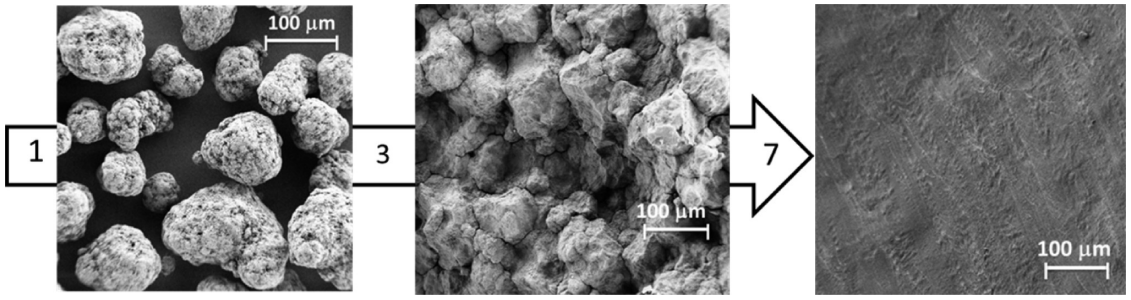

Figure 4. SEM micrographs at three steps of sintering: (left) nascent powder prior to compaction at step 1; (center) fracture surface of a densified sample at step 3; (right) fracture surface of a sintered sample at step 7 (15 min, 150 °C).

mechanisms of sintering, i.e., chain re-entanglement and cocrystallization.

The SEM micrographs of Figure 4 show that the particle morphology is fairly spherical. During the stage of densification, the powder grains exhibit excellent surface contact that will be next corroborated by density and SAXS measurements. The faceted grains reveal a high level of plastic deformation that is mandatory to rule out porosity and ensure perfect surface contact and wetting of the powder particles. However, the brittle-like fracture propagating along the grain interfaces clearly show that these grains kept their integrity during the densification stage below the melting point, with no molecular diffusion at interfaces.

Density measurements after precompaction were very close to 0.93 g/cm^3. Considering that crystallinity was about 58%, according to DSC data, this result indicates insignificant remaining porosity; i.e., densification was correctly performed to ensure good wetting of the powder grains.

The missing of small-angle X-ray scattering at very low scattering angle about the beam stop confirmed the absence of porosities in the size range 1−60 nm.

Considering the above conclusions from density, SAXS and SEM, it is assumed that the powder particle wetting after the precompaction stage is nearly perfect without any chain interdiffusion. Thereby, only the effect of the sintering time and temperature on the particle welding has been studied via tensile tests, the pressure cycle during the sintering process being the same for all the samples.

Tensile Testing above the Melting Point. Figures 5 and 6 display plots of true stress−strain curves for various sintering conditions. Every stress−strain curve displayed on these plots is a representative curve among four independent tensile tests.

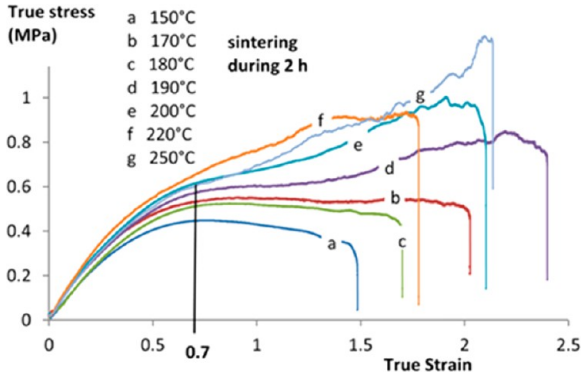

Figure 5. True stress−strain tensile curves at a draw temperature T_d =150 °C for a sintering time t_s = 2 h for different values of the sintering temperature, T_s, given in the legend.

Figure 5 shows the true stress−strain tensile curves at the draw temperature T_d = 150 °C for a sintering time t_s = 2 h for different values of the sintering temperature, T_s. These tensile curves exhibit two different types of behavior: (i) without strain hardening for sintering performed at low temperature (curves a−c); (ii) with strain hardening for sintering performed at higher temperature (curves d−g).

Moreover, the elastic modulus and the elongation at break also exhibit an increasing trend with increasing T_s, the dispersion being rather great on the second parameter. This is a qualitative hint of an improvement of the interparticle cohesion associated with chain interdiffusion including chain re-entanglement at the interface of the powder particles.

Figure 6 shows the true stress−strain curves for samples sintered at T_s = 150 °C and T_s = 200 °C for different sintering times, t_s. For the sintering at T_s = 150 °C (Figure 6a), the evolution of the stress−strain curves is similar to that of the preceding case with two types of behavior: without strain hardening for the short sintering times and with strain hardening for long sintering times. In contrast, for a sintering at T_s = 200 °C (Figure 6b), all stress−strain curves exhibit strain hardening, regardless of t_s. Moreover, all curves are surprisingly almost superposed for sintering durations in the range 15 min < t_s < 100 h. Figures 6a,b show that t_s has a rather weak influence on sintering compared with temperature: the higher T_s, the lower the t_s influence.

Three mechanical parameters have been analyzed for probing more specifically the evolution of chain interdiffusion as a function of sintering time and temperature, the pressure cycle during the process being the same for all samples (see Figure 1): the elastic modulus, E, the stress at a strain level ε = 0.7 in the pseudoplateau region, σ_{pp}, and the strain recovery after rupture, R.

Experimental data regarding the elastic modulus and the stress at pseudoplateau are reported in Figures 7 and 8 for every sintering and drawing conditions. The data are plotted on ln/ln graphs in consideration of a theoretical approach involving a power law that will be later discussed in the Discussion subsection. The data points refer to average values of four independent measurements. The error bars hold for the extent of the data dispersion between the highest and the lowest experimental values. A rather high dispersion of the data can be observed that makes difficult the determination of evolution trends, more particularly regarding the modulus data. This data dispersion is supposed to result from some statistical welding defects due to very local imperfect wetting of the powder particles. Moreover, elastic modulus measurements are rather

dx.doi.org/10.1021/ma402012f | Macromolecules 2014, 47, 197−207

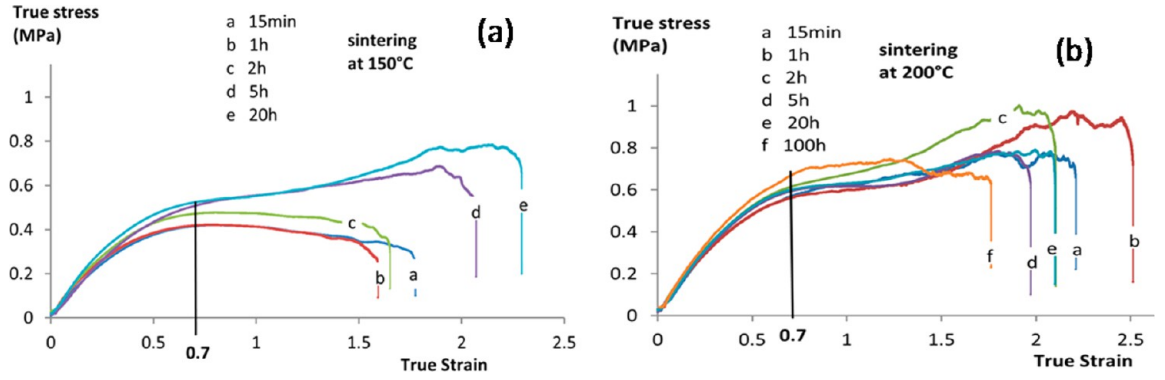

Figure 6. True stress−strain curves at T_d = 150 °C for a sintering at (a) T_s = 150 °C and (b) T_s = 200 °C during different sintering times, t_s, given in the legend.

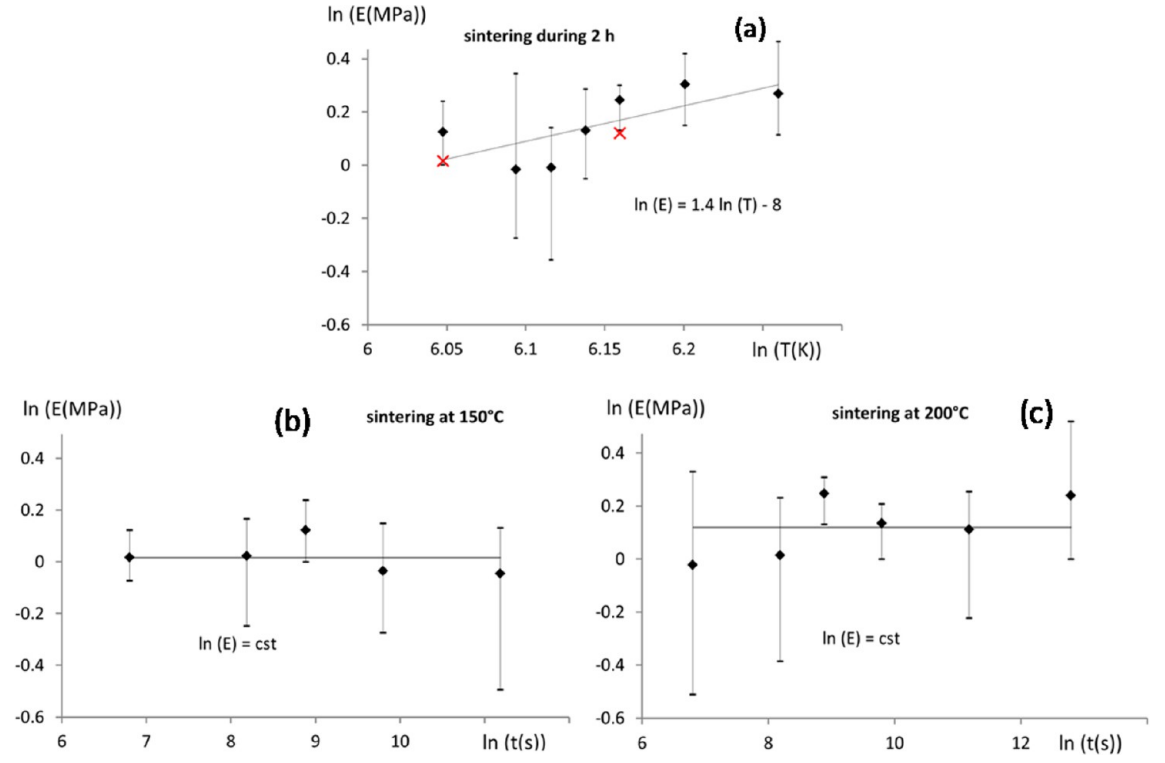

Figure 7. Elastic modulus at T_d = 150 °C (a) as a function of temperature of sintering for t_s = 2 h and as a function of sintering time (b) for T_s = 150 °C and (c) for T_s = 200 °C (data from Figures 4 and 5). Note that the two red crosses are average values taken from (b) and (c).

tricky due to difficulties in the clamping and preloading of the samples that introduce nonsystematic uncertainties in the stress−strain curves at the onset of straining.

For that reason, the data have been analyzed by means of statistical tests in order to determine the regression lines and the corresponding slopes in Figures 7 and 8. A detailed description of this method is given in the Supporting Information.

In the present approach, the elastic modulus, E, is a relevant parameter of the UHMWPE deformation in the molten state since it can be directly related to the entanglement density of the macromolecular network in the framework of the theory of rubber elasticity via the following equation giving the initial slope of the stress−strain curve:[28]

$$E = 3\frac{\rho RT}{M_e} \quad (2)$$

where ρ is the material density, R the gas constant, and M_e the molecular mass between entanglements.

Figure 7a shows that the elastic modulus follows a clearly positive evolution with the increase of the sintering temperature despite significant dispersion of the experimental data. In contrast, Figures 7b,c show no evolution of the elastic modulus with sintering time for both values of the sintering temperature.

The extremum values of the elastic modulus taken from Figure 7a are 1.0 and 1.3 MPa for 150 < T_s < 250 °C. According to eq 2 and taking the density of molten PE as ρ = 0.855 g/cm^3, these data reveal a decrease of M_e from 9000 to 7000 g/mol with increasing T_s. This is a piece of evidence of (1) an actual chain re-entanglement during the sintering process and (2) a benefiting effect of increasing T_s far beyond the melting point. However, comparing these data with the value 1200 < M_e < 2500 g/mol for molten PE at equilibrium[29−32] clearly indicates that chain re-entanglement

dx.doi.org/10.1021/ma402012f | Macromolecules 2014, 47, 197−207

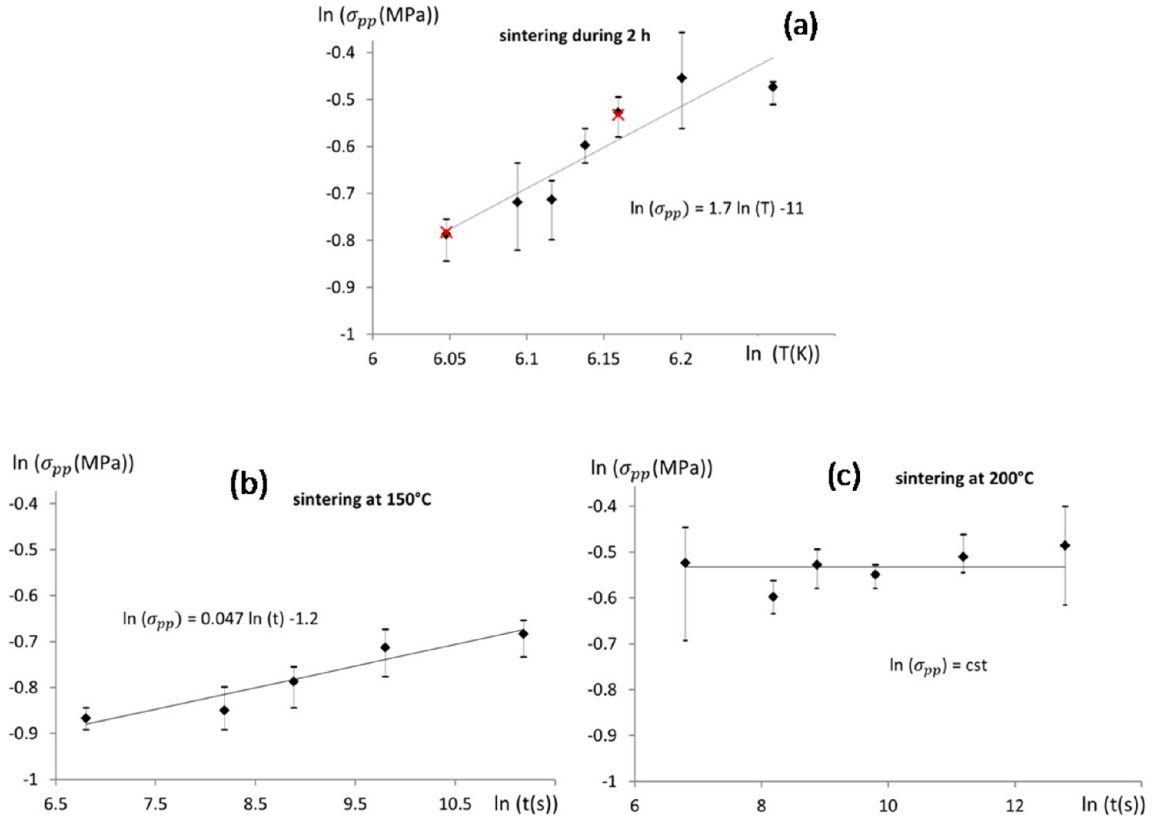

Figure 8. Stress at pseudoplateau at T_d = 150 °C (a) as a function of temperature of sintering for t_s = 2 h and as a function of time of sintering (b) for T_s = 150 °C and (c) for T_s = 200 °C (data from Figures 4 and 5). Note that the two red crosses are values taken from interpolations on (b) and (c).

is only partial for UHMWPE for sintering 2 h above T_m. Moreover, the nondependence on time is a quite surprising observation with regard to the common processes of polymer diffusion. This point will be further discussed in the Discussion subsection.

The stress, σ_{pp}, measured at a true strain ε = 0.7 in the pseudoplateau region is another relevant parameter in this study. Besides being more easily measurable than the elastic modulus, this parameter displays lower data dispersion as can be seen in Figure 8 despite very low values in the range 0.4−0.7 MPa, depending on the sintering and drawing conditions. According the rubber elasticity theory, this parameter should obey the relation[28]

$$\sigma = \frac{\rho RT}{M_e}\left(\lambda^2 - \frac{1}{\lambda}\right) \quad (3)$$

which means that at given strain and draw temperature, an increase of stress can be assigned to a M_e decrease, i.e., an increase of chain re-entanglement in relation to processing conditions.

However, during the tensile tests, some chain disentanglement is likely to occur in the sintered samples. Therefore, the stress at pseudoplateau cannot be directly connected to the actual entanglement density, but it is worth being used as a qualitative and comparative indicator of chain re-entanglement during sintering.

The data displayed in Figure 8 show a very clear increase of σ_{pp} with the increase of sintering temperature (Figure 8a) and little sensitivity of to sintering time (Figures 8b,c). This finding perfectly corroborates the observation from the tensile modulus data of a significant increase of chain re-entanglement with increasing T_s (Figure 8a). However, in Figure 8b σ_{pp} seems to weakly increase with increasing t_s for T_s = 150 °C, whereas Figure 8c shows no evolution of σ_{pp} with t_s for T_s = 200 °C. This is a hint that interfacial healing is somewhat slower at T_s = 150 °C as compared with T_s = 200 °C and that further chain re-entanglement can occurs beyond the time of the present experiments due to partial contribution of very slow reptation motions.

At first sight, the σ_{pp} evolution with time seems to be slightly different from that of the elastic modulus for the two sintering temperatures. However, the statistical analysis (see Supporting Information) enables to affirm that the σ_{pp} evolution with T_s is much different from that with t_s at 150 °C. As a matter of fact, the slope of the T_s dependence regression is about 36 times higher than that of the t_s dependence (see Figures 8a,b).

It results from the statistical analysis that the pseudoplateau stress is sintering temperature depend but displays very low sensitivity to sintering time, at T_s close to the melting point. Besides, the σ_{pp} increase with increasing T_s thoroughly confirms the conclusion from the modulus data analysis of an improvement of chain re-entanglement.

Strain recovery was the third mechanical parameter to be used for checking the state of entanglement of the molecular network. Indeed, upon unloading, an un-cross-linked rubber network is likely to undergo two contradictory phenomena, i.e., entropic strain recovery and liquid-like flow. This should result in a dependence of strain recovery on entanglement density. The statistical analysis of the unreported data regarding the sintered sample recovery after stretching up to rupture showed a positive dependence on sintering temperature, i.e., the higher

dx.doi.org/10.1021/ma402012f | Macromolecules 2014, 47, 197−207

T_s, the better the recovery. This gives clear indication of an increase of chain re-entanglement with increasing T_s. However, no significant dependence on the sintering time was observed.

The three mechanical parameters, i.e. elastic modulus, pseudoplateau stress, and strain recovery, exhibit a clear dependence on the sintering temperature but no significant sensitivity to the sintering time up to 100 h. This finding surprisingly disagrees with the classical reptation theory which has been often claimed to account for the welding or healing of polymers interfaces[6−10] and which predicts similar dependence on time and temperature. This point will be further discussed in the Discussion subsection.

Tensile Testing at Room Temperature. Mechanical tests of the solid sintered materials give information on the strength of the particles interface including the contributions of both the interdiffusion of the chains emanating from the jointing particles and the cocrystallization of these chains. Even though a major role has been attributed to cocrystallization on the efficiency of polymer welding,[11−13] it is to be noticed that very few direct experimental evidences have been provided.[33]

The stress−strain curves recorded at RT are reported in Figures 9 and 10. It is worth noticing that the tensile modulus

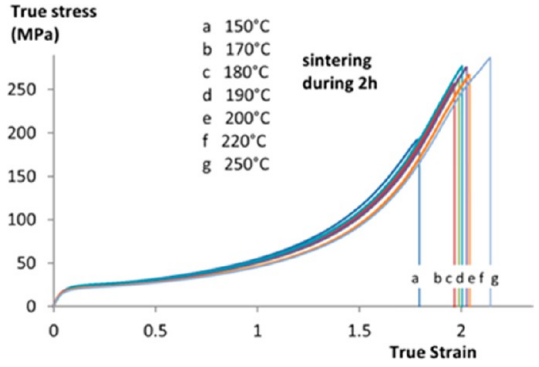

Figure 9. True stress−strain tensile curves at room temperature for a sintering time t_s = 2 h at different sintering temperatures given in the legend.

and the yield stress are little dependent on sintering conditions. This may be understood by the fact that both parameters are mainly dependent on the crystallinity index of semicrystalline polymers that is very similar for all the sintered samples of the present study, irrespective of sintering conditions. This observation emphasizes the huge role of cocrystallization at the particle interface that significantly hides the much fainter mechanical effect of re-entanglement. As a matter of fact, cocrystallization can take place after chain interdiffusion over distances shorter than that required for re-entanglement. Note that similar conclusion has been made by Doucet et al.[16] Besides, the enthalpic cohesion of crystals requires much higher stress level for deformation compared to the entropic like forces involved in network stretching.

Notwithstanding, the elongation at break in the solid state seems to depend on the sintering time for T_s = 150 °C (Figure 10a), whereas it does not depend for T_s = 200 °C (Figure 10b). It is well-known[28] that the strain at break of cross-linked polymer networks in the rubbery state is directly connected to the entanglement density through the relation $\lambda_{max} \propto N_e^{1/2}$, where N_e is the chain length between entanglements (including cross-links) given in number of random links. This was shown to fairly apply to the elongation at break of various semicrystalline polymer networks including UHMWPE.[34−41] In the present study, it is likely that for sintering at 150 °C, healing by interface re-entanglement would not be completed at 150 °C. As a consequence the crystalline network could hide any difference until fracture, but near the fracture the material is expected to be more sensitive to the possible weakness of the entanglement network.

To sum up, the tensile data at RT corroborate the previous observations from the drawing behavior at T_d = 150 °C that sintering is only slightly sensitive to sintering time at T_s = 150 °C and no longer at T_s = 200 °C.

Discussion on the Re-entanglement Kinetics. The dual mechanical approach of tensile testing above and below the melting temperature was aimed at discriminating the role on the interfacial cohesion due to the chain re-entanglement from the contribution of cocrystallization. It appeared that cocrystallization has a tremendous role on the mechanical strength at room temperature even for very short sintering time. This point has been claimed in studies dealing with welding or interface healing of semicrystalline polymers, yet with very few if any experimental evidence. On the other hand, the mechanical tests carried out above the melting point enabled us to focus on the very mechanism of chain intertwining during the sintering process.

Welding of polymer parts or sintering of polymer powders is a diffusive process that has been theoretically approached by assuming that the polymer chains have to diffuse across the interface(s) following a mechanism analogous to polymer reptation[6−9] as depicted in Figure 11. Indeed, the kinetics for

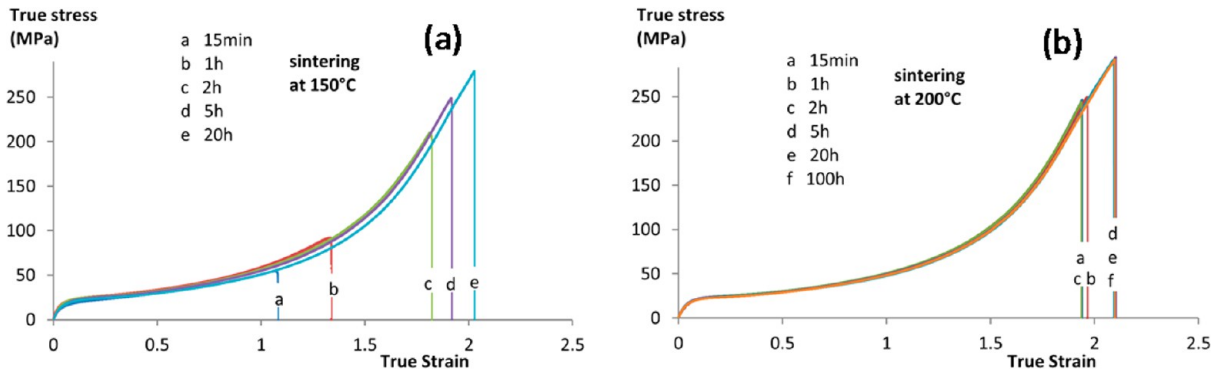

Figure 10. True stress−strain curves at RT for a sintering at (a) T_s = 150 °C and (b) T_s = 200 °C during different sintering times given in the legend.

dx.doi.org/10.1021/ma402012f | Macromolecules 2014, 47, 197−207

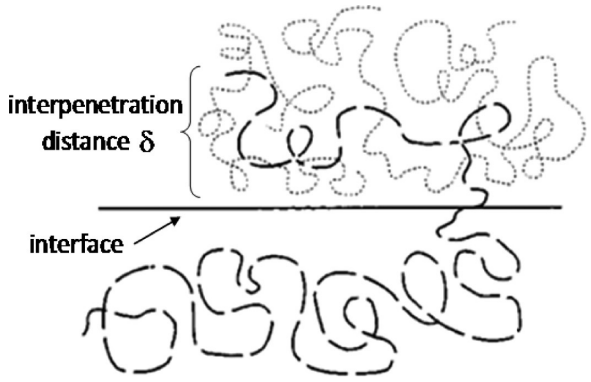

Figure 11. Sketch of chain diffusion across an interface according to ref 3.

the interfacial strength to reach the bulk material property is supposed to be identical to that of chains to restore their reptation tube. The characteristic reptation time of a polymer chain, τ_{rep}, that is the time necessary for the chain to completely escape from its initial tube[3,4] is given by the relation[5]

$$\tau_{rep} = \frac{\zeta N^3 b^4}{\pi^2 e^2 k_B T} \quad (4)$$

where ζ is the monomeric friction coefficient, N the number of monomers, b the effective bond length, e the mesh size of the entangled network, k_B the Boltzmann constant, and T the temperature. The memory of the initial conformation is then completely lost, and the chain enters randomly in a new tube. In this theory, the chains are modeled by a series of entropic springs whose restoring force is proportional to temperature. The reptation time is thus inversely proportional to the temperature.

In the framework of this theory, the dependence on time, t, of the interpenetration distance of a chain across an interface, δ, obeys the relation[1,3]

$$\delta \propto \left(\frac{t}{\tau_{rep}}\right)^{\gamma} \quad (5)$$

By combining eqs 4 and 5, and assuming temperature-independent ζ, it comes that

$$\delta \propto (tT)^{\gamma} \quad (6)$$

which means that the δ distance has the same dependence on time and temperature.

The first striking experimental observation is that a highly cohesive molten material is obtained within about a dozen of minutes even for the lowest temperature. It seems to be in contradiction with the classical reptation theory. Indeed, at 150 °C the reptation time is $\tau_{rep} \approx 2$ h for chains having a molecular mass of 3900 kg/mol,[42] so that the healing should be very imperfect in the present case. To explain this observation, it has first to be noticed that it is likely that chains do not need to diffuse completely over their whole length to provide good mechanical properties to the material. In a recent theoretical approach of polymer fracture based on a rigidity percolation model, Wool[43] predicted that fracture by chain disentanglement of glassy or semicrystalline polymers will only occur in the molecular weight range $M_c < M < 8M_c$, where $M_c \approx 2M_e$ is the critical molecular weight of entanglement. In this M range, G_{1C} scales as $[(M/M_c)^{1/2} - 1]^2$. For $M > 8M_c$, the fracture will occur by chain scission at constant value $G_{1C} = G^{\circ}_{1C}$. This applies to the healing of polymer interfaces as well. It means that polymers having chains longer than $8M_c$ would only have to diffuse over a distance close to $8M_c$ along their reptation tube for the completion of the healing or the welding of polymer interfaces. In the present case of PE, the threshold value is $8M_c \approx 40\,000$ g/mol.[29−31]

However, if this limitation could possibly justify the time scale of interface healing, it does not seem to be sufficient to explain the mechanical properties. Indeed, if we consider that a typical UHMWPE ($\tau_{rep} \approx 2$ h) could diffuse by chain-end motion over a distance of about $8M_c$ within a very a short sintering time, and if we consider the optimistic hypothesis that all the chain ends are able to diffuse in an adjacent powder particle, then the two segments of $8M_c$ per chain biding two adjacent particles represent only 1% of the volume of the material of an UHMWPE of 3900 kg/mol according to the scheme of Figure 12. Therefore, only 1% of the matter in the interfacial region would contribute significantly to transfer the forces through the interface, which would lead to a stress concentration of at least a factor 100. Significant cracks would appear between the anchoring points and would entail brittleness.

It is then more realistic to imagine that the whole part of the chain between chain ends could also intertwine with neighbor chains by diffusion mechanisms and then could contribute, at least partially, to the interface reinforcement even for short

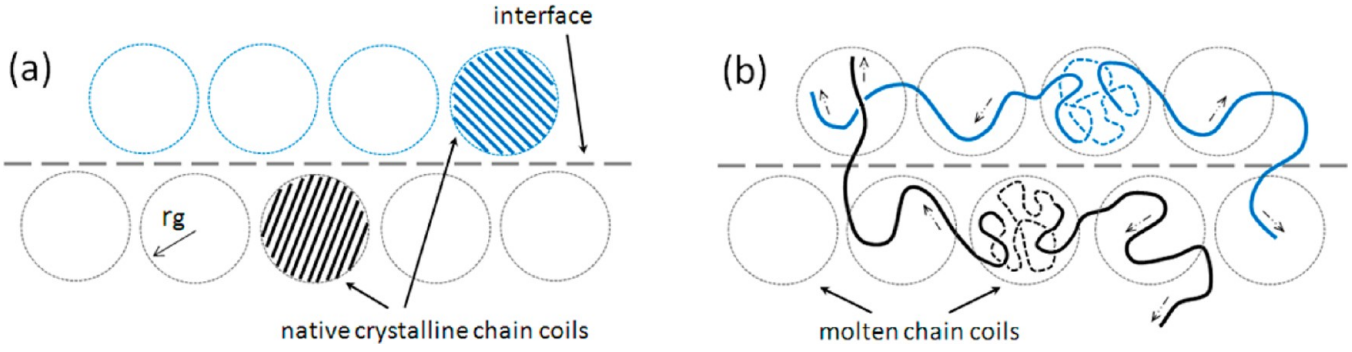

Figure 12. Schematic of the interfacial chain diffusion via chains ends: (a) after precompaction polymer chains are densely packed along the particle interface in the form of highly crystalline entities (native crystals) with a characteristic $r_g \ll R_g$ (random coil); (b) during sintering the molten chain coils undergo a slow reptation-like diffusion that allows intertwining with the neighboring coils; some of the chain ends may experience migration through the interface.

dx.doi.org/10.1021/ma402012f | Macromolecules 2014, 47, 197−207

sintering time. Indeed, the present experimental results are quite consistent with previous studies regarding the welding of disentangled UHMWPE solution-crystallized samples which showed that bulk properties are recovered much faster than predicted by the polymer reptation theory, according to Barham and Sadler[42] as well as Bastiaansen et al.[44] and Xue et al.[14] These authors suggested that the relevant mechanism of chain re-entanglement in such disentangled systems is likely to involve "sideways motions" or "segmental rather to macromolecular mobility" at the scale of the gyration radius or nearly so, i.e., about 40 times greater than the end-to-end distance between entanglements in the present instance of UHMWPE. De Gennes[45] proposed a theoretical approach based on cooperative Rouse motions of disentangled chains that fairly accounts for the experimental data. The mechanism of chain intertwining via the so-called *melting explosion* is sketched in Figure 13 for the present situation of native powder sintering.

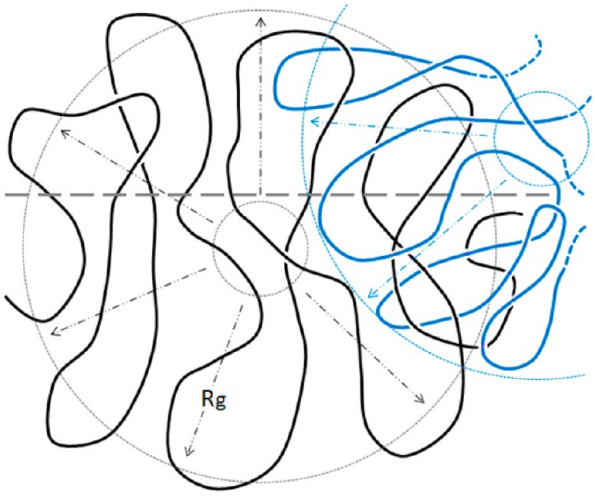

Figure 13. Schematic of the interfacial chain diffusion via *melting explosion*: the chain coils undergo a sudden change of gyration radius from r_g to R_g; very quick migration of some chain loops and chain ends through the interface enables chain overlap over a distance largely exceeding $8M_c$.

The kinetics of such motions could be moreover very quick. Indeed, these specific materials can take benefit from their nonequilibrium initial state. It has been proposed that chain intertwining from disentangled solution-crystallized samples of UHMWPE essentially relies on the phenomenon of *melting explosion*.[14,42,44] The regular chain-folded structure of UHMWPE single crystals grown from solution is such that radius of gyration, R_g, is much lower than that of the corresponding random coil. However, after quick melting for only a few seconds and subsequent recrystallization, R_g of the recrystallized the chain proved to be close to the value predicted from the conventional statistics of polymer chains as demonstrated by Barham and Sadler.[42] This means that the chains having a compact nonequilibrium conformation in solution-crystallized UHMWPE can reach an equilibrium trajectory in a time scale considerably shorter than the reptation time. This entropy-driven phenomenon has been called *melting explosion* owing to both the huge R_g change and the fastness of the phenomenon.[45] The thermodynamic force for *melting explosion* is even stronger as the chain is well folded in the disentangled crystal and the chain length is high (great R_g difference between crystal and melt). Even for bulk material this thermodynamic force exists and helps chains to intertwine at the interfaces. In the present study, UHMWPE nascent powders are known to be partially disentangled, highly crystalline, and the chains are very long. In these circumstances, chain diffusion would occur in a time scale much shorter than predicted from a reptation regime, which is actually observed.

In order to verify the assumption that *melting explosion* is of prime importance for nascent powder sintering, a part of nascent powder has been premelted prior to sintering, taking care that the powder grains remain separated one from each other during the melting treatment. The aim was to decrease strongly the *melting explosion* thermodynamic force by achieving a prior re-entangling in each powder particle so that subsequent melting will not entail significant *melting explosion*. This experimental approach borrows from the study reported by Xue et al.[14] regarding solution-crystallized UHMWPE. Sintering was thus performed using the so-called premelted powder for 15 min at 150 °C, i.e., the sintering conditions that enable to produce a fairly cohesive material in very short time in the case of the nascent powder. The stress–strain curves of Figure 14 show that the material produced by sintering of the premelted powder has considerably lower mechanical characteristics than the one produced with the nascent powder.

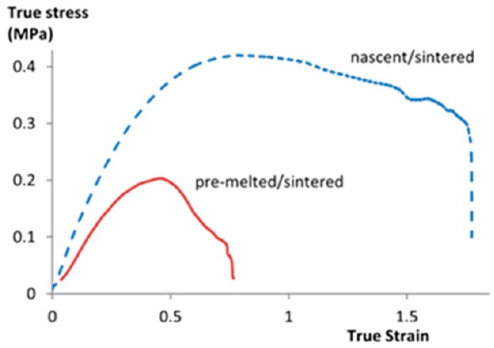

Figure 14. Stress–strain curves at 150 °C of UHMWPE sintered samples using either a nascent or a premelted powder (sintering conditions: 150 °C, 15 min).

This means that if *melting explosion* is achieved prior to the sintering process, it prevents efficient welding of the powder particles. This experiment provides a piece of evidence that *melting explosion* does play a determining role in the efficiency of the nascent powder sintering.

Considering the weak and yet substantial strength of the premelted powder after a sintering time of 15 min only, it is likely that the sintering process occurred via interdiffusion over short distances of segmental motions between entanglements in substitution to the reptation at such short time, according to the mechanism described by Wool and co-workers for equilibrium entangled polymers.[46,47] This kind of mechanism should be insignificant in comparison to the *melting explosion* process for the sintering of the native powder due to the nonequilibrium chain topology and the lacking of chain entanglements.

The second surprising observation concerns the relative influence of sintering time and temperature on the mechanical properties. The experimentally observed variations with time and temperature of the elastic modulus, the pseudoplateau

dx.doi.org/10.1021/ma402012f | *Macromolecules* 2014, 47, 197–207

stress, and the strain recovery are quite different: the slopes of the ln/ln plots of Figures 7a and 8a show that the power factor of eq 6 is $\gamma = 1.4$ or 1.7 regarding the temperature dependence of E or σ_{PP}, respectively, and is $\gamma \leq 0.05$ for the time dependence. This finding is again contradictory with a classical reptation-governed diffusion process (eq 6) during sintering.

After melting explosion chain segments have been rapidly expelled in all directions from the initial crystal. It is then likely that chain segments that have diffused across the interfaces are only partially entangled. Moreover, the interpenetration distance could remain still insufficient. Then the perfect interface healing should be reached when both the interpenetration distance is high enough and when the chain segments are well re-entangled. This evolution toward equilibrium takes places via chain motions which were observed to be much more sensitive to temperature than time as if it was thermally activated. This observation could be accounted for in the framework of reptation considering the temperature dependence of the friction coefficient of eq 4 that was assumed to be constant in eq 6. Indeed, several authors have clearly pointed out the strong ζ-dependence on temperature[48,49] that is unfortunately often ignored.[5] This ζ temperature dependence that applies for reptation should also apply for "sideways motions" or "segmental rather to macromolecular mobility" which are likely to contribute to interface healing after melting explosion.

CONCLUSION

A sintering protocol of UHMWPE nascent powder was developed with two variable parameters: time and temperature. The sintered samples were mechanically tested at room temperature and in the rubbery temperature domain that allowed studying separately the role on the consolidation process of re-entanglement and cocrystallization. We have clearly shown that at room temperature the crystalline network is the dominant parameter compared to entanglement network. Indeed, in the solid state, the cocrystallization enables to quickly reach good mechanical properties at rather short sintering time close to the melting point. Besides, solid state properties reach roughly constant value at much shorter sintering time than in the case of the molten state. This can be assigned to the high cohesiveness of the crystals that bridles the macromolecules network even in the case of very little interfacial diffusion of chains.

Regarding the behavior above the melting point, the first striking result is that the mechanical properties in the rubbery state (without any cocrystallization) reach significant value even for very short sintering time compared to reptation time. This result appears to be in contradiction with classical interdiffusion theory based on reptation concepts. In the case of UHMWPE, this can be explained by considering the role of the *melting explosion* phenomenon that strongly enhanced the diffusion of chain segments. This phenomenon has been first proposed for solution-crystallized samples, and in the present work, it was shown to occur also for nascent UHMWPE powders. During the *melting explosion* process, the intertwining of chains from neighbor particles by sideway motions of initially disentangled chain loops is much faster than the reptation of chains by both ends along their tube. This mechanism promotes the recovery of bulk properties within a time scale much shorter than the reptation time in the case of very long chains. The observation that some properties do not completely level off after 100 h of sintering strongly suggests that the contribution of reptation for very long sintering times should not be excluded.

It has also been given evidence that the mechanism of sintering is much more dependent on temperature than time. This does not agree with classical reptation theory that predicts the same dependence on both parameters, and which is known to apply for the welding or crack healing of short chain polymers. Diffusion by chain ends and sideways motions are probably involved in the healing of very long chains polymer interfaces to reach a sufficiently high entanglement density in the interfacial zone. It is our hypothesis that whatever the diffusion mechanisms, i.e. reptation or sideways motions, it should be strongly sensitive to the friction coefficient that is much sensitive to temperature but for which no explicit formulation exists in the literature.

ASSOCIATED CONTENT

Supporting Information

Figures A–C. This material is available free of charge via the Internet at http://pubs.acs.org.

AUTHOR INFORMATION

Corresponding Author

*E-mail olivier.lame@insa-lyon.fr (O.L.).

Notes

The authors declare no competing financial interest.

ACKNOWLEDGMENTS

The authors are indebted to Ticona (Oberhausen, Germany) for the generous supply of the UHMWPE sample together with its molecular characteristics.

REFERENCES

(1) Kim, Y. H.; Wool, R. P. A theory of healing at a polymer interface. *Macromolecules* **1983**, *16*, 1115–1120.

(2) Al Jebawi, K.; Sixou, B.; Vigier, G.; Seguela, R. Hot compaction of polyoxymethylene. Part 1: Processing and mechanical evaluation. *J. Appl. Polym. Sci.* **2006**, *102*, 1274–1284.

(3) Bousmina, M.; Qiu, H.; Grmela, M.; Klemberg-Sapieha, J. E. Diffusion at polymer/polymer interfaces probed by rheological tools. *Macromolecules* **1998**, *31*, 8273–8280.

(4) (a) de Gennes, P.-G. Reptation of a polymer chain in the presence of fixed obstacles. *J. Chem. Phys.* **1971**, *55*, 572–579. (b) de Gennes, P.-G. *Scaling Concepts in Polymer Physics*; Cornell University Press: Ithaca, NY, 1979.

(5) Doi, M.; Edwards, S. F. *The Theory of Polymer Dynamics*: Oxford Science Publications: Oxford, UK, 1986.

(6) Jud, K.; Kausch, H.-H.; Williams, J. G. Fracture mechanics studies of crack healing and welding of polymers. *J. Mater. Sci.* **1981**, *16*, 204–210.

(7) Prager, S.; Tirrell, M. The healing process at polymer-polymer interfaces. *J. Chem. Phys.* **1981**, *75*, 5194–5198.

(8) Wool, R. P.; O'Connor, K. M. A theory of crack healing in polymers. *J. Appl. Phys.* **1981**, *52*, 5953–5963.

(9) (a) de Gennes, P.-G. *C. R. Acad. Sci. Paris, Ser. B* **1980**, *291*, 219–221. (b) de Gennes, P.-G. The formation of polymer/polymer junctions. *Tribol. Ser.* **1982**, *7*, 355–367.

(10) Yuan, B.-L.; Wool, R. P. Strength development at incompatible semicrystalline polymer interfaces. *Polym. Eng. Sci.* **1990**, *30*, 1454–1464.

(11) Gent, A. N.; Kim, E.-G.; Ye, P. Auto-adhesion of crosslinked polyethylene. *J. Polym. Sci., Polym. Phys.* **1997**, *35*, 615–622.

(12) Xue, Y.-Q.; Tervoort, T. A.; Rastogi, S.; Lemstra, P. J. Welding behavior of semicrystalline polymers. 2. Effect of cocrystallization on auto-adhesion. *Macromolecules* **2000**, *33*, 7084–7087.

(13) Frederix, C.; Beauchene, P.; Seguela, R.; Lefebvre, J.-M. Kinetics of the fusion-welding of unlike ethylene-copolymers over a wide crystallinity range. *Polymer* **2013**, *54*, 2755−2763.
(14) Xue, Y.-Q.; Tervoort, T. A.; Lemstra, P. J. Welding Behavior of Semicrystalline Polymers. 1. The effect of nonequilibrium chain conformations on autoadhesion of UHMWPE. *Macromolecules* **1998**, *31*, 3075−3080.
(15) Jauffres, D.; Lame, O.; Vigier, G.; Dore, F. Microstructural origin of physical and mechanical properties of ultra high molecular weight polyethylene processed by high velocity compaction. *Polymer* **2007**, *48*, 6374−6383.
(16) Doucet, N.; Lame, O.; Vigier, G.; Dore, F.; Seguela, R. Sintering kinetics of UHMWPE nascent powders by high velocity compaction: Influence of molecular weight. *Eur. Polym. J.* **2013**, *49*, 1654−1661.
(17) Jauffrès, D.; Lame, O.; Vigier, G.; Doré, F.; Douillard, T. Sintering mechanisms involved in high-velocity compaction of nascent semicrystalline polymer powders. *Acta Mater.* **2009**, *57*, 2550−2559.
(18) Xiong, B.; Lame, O.; Chenal, J.-M.; Rochas, C.; Seguela, R.; Vigier, G. In-situ SAXS study and modeling of the cavitation/crystal-shear competition in semi-crystalline polymers: Influence of temperature and microstructure in polyethylene. *Polymer* **2013**, *54*, 5408−5418.
(19) Etienne, S.; Cavaille, J.-Y.; Perez, J.; Point, R.; Salvia, M. Automatic system for analysis of micromechanical properties. *Rev. Sci. Instrum.* **1982**, *53*, 1261−1266.
(20) Chanzy, H. D.; Bonjour, E.; Marchessault, R. H. Nascent structures during the polymerization of ethylene. II. Calorimetric study. *Colloid Polym. Sci.* **1974**, *252*, 8−14.
(21) Smith, P.; Chanzy, H. D.; Rotzinger, B. P. Drawing of virgin ultrahigh molecular weight polyethylene: an alternascent route to high strength/high modulus materials. Part 2. Influence of polymerization temperature. *J. Mater. Sci.* **1987**, *22*, 523−531.
(22) Rotzinger, B. P.; Chanzy, H. D.; Smith, P. High strength/high modulus polyethylene: synthesis and processing of ultra-high molecular weight virgin powders. *Polymer* **1989**, *30*, 1814−1819.
(23) Loos, J.; Arndt-Rosenau, M.; Weingarten, U.; Kaminsky, W.; Lemstra, P. J. Melting behavior of nascent polyolefins synthesized at various polymerization conditions. *Polym. Bull.* **2002**, *48*, 191−198.
(24) Joo, Y. L.; Han, O. H.; Lee, H.-K.; Song, J. K. Characterization of ultra high molecular weight polyethylene nascent reactor powders by X-ray diffraction and solid state NMR. *Polymer* **2000**, *41*, 1355−1368.
(25) Rastogi, S.; Lippits, D. R.; Peters, G. W. M.; Graft, R.; Yao, Y.; Spiess, H. W. Heterogeneity in polymer melts from melting of polymer crystals. *Nat. Mater.* **2005**, *4*, 635−641.
(26) Rastogi, S.; Lippits, D. R.; Höhne, G. W. H.; Mezari, B.; Magusin, P. C. M. M. The role of the amorphous phase in melting of linear UHMWPE: Implications for chain dynamics. *J. Phys.: Condens. Matter* **2007**, *19*, 205122/1−21.
(27) Jauffrès, D.; Lame, O.; Vigier, G.; Doré, F. How nascent structure of semicrystalline polymer powders enhances bulk mechanical properties. *Macromolecules* **2008**, *41*, 9793−9801.
(28) Treloar, L. R. G. *The Physics of Rubber Elasticity*, 2nd ed.; Oxford University Press: Oxford, UK, 1975.
(29) Porter, R. S.; Johnson, J. F. Entanglement concept in polymers. *Chem. Rev.* **1966**, *65*, 1−27.
(30) Doi, M.; Edwards, S. F. Dynamics of concentrated polymer systems. Part 3. The constitutive equation. *J. Chem. Soc., Faraday Trans. 2* **1978**, *74*, 1818−1832.
(31) Aharoni, S. M. On entanglements of flexible and rodlike polymers. *Macromolecules* **1983**, *16*, 1722−1728.
(32) Liu, C.; He, J.; van Ruymbeke, E.; Keunings, R.; Bailly, C. Evaluation of different methods for the determination of the plateau modulus and the entanglement molecular weight. *Polymer* **2006**, *47*, 4461−4479.
(33) Schuman, T.; Stepanov, E. V.; Nazarenko, S.; Capaccio, G.; Hiltner, A.; Baer, E. Interdiffusion of linear and branched polyethylene in microlayers studied via melting behavior. *Macromolecules* **1998**, *31*, 4551−4561.
(34) Kanamoto, T.; Sherman, E. S.; Porter, R. S. Extrusion of polyethylene single crystals. *Polym. J.* **1979**, *11*, 497−502.
(35) (a) Smith, P.; Lemstra, P. J. Ultra high strength polyethylene filaments by solution spinning-drawing. III. Influence of drawing temperature. *Polymer* **1980**, *21*, 1341−1343. (b) Smith, P.; Lemstra, P. J.; Booij, H. C. Ultradrawing of high-molecular-weight polyethylene cast from solution. II. Influence of initial polymer concentration. *J. Polym. Sci., Polym. Phys.* **1981**, *19*, 877−888.
(36) Matsuo, M.; St John Manley, R. Ultra-drawing at room temperature of HMWPE. *Macromolecules* **1982**, *15*, 985−987.
(37) Peguy, A., St; John Manley, R. Ultra-drawing of high molecular weight polypropylene. *Polym. Commun.* **1984**, *25*, 39−42.
(38) Gogolewski, S.; Pennings, A. J. High modulus fibers of nylon6 prepared by a dry-spinning method. *Polymer* **1985**, *26*, 1394−1400.
(39) Cebe, P.; Grubb, D. Gel-drawn fibers of poly(vinyl-alcohol). *J. Mater. Sci.* **1985**, *20*, 4465−4478.
(40) Ito, M.; Tanaka, K.; Kanamoto, T. Effects of initial morphology and molecular weight on the drawability of poly-ethylene-terephthalate. *J. Polym. Sci., Polym. Phys.* **1987**, *25*, 2127−2138.
(41) Bastiaansen, C. W. M. Influence of initial polymer concentration in solution and weight-average molecular weight on the drawing behavior of polyethylenes. *J. Polym. Sci., Polym. Phys.* **1990**, *28*, 1475−1482.
(42) Barham, P. J.; Sadler, D. M. A neutron scattering study of the melting behaviour of polyethylene single crystals. *Polymer* **1991**, *32*, 393−395.
(43) (a) Wool, R. P. Rigidity percolation model of polymer fracture. *J. Polym. Sci., Polym. Phys.* **2005**, *43*, 168−183. (b) Wool, R. P. Adhesion at polymer-polymer interfaces: a rigidity percolation approach. *C. R. Chim.* **2006**, *9*, 25−44.
(44) Bastiaansen, C. W. M.; Meyer, H. E. H.; Lemstra, P. J. Memory effects in polyethylenes: influence of processing and crystallization history. *Polymer* **1990**, *31*, 1435−1440.
(45) de Gennes, P.-G. Explosion à la fusion (Explosion upon melting). *C. R. Acad. Sci., Ser. 2* **1995**, *321*, 363−365.
(46) (a) Zhang, H.; Wool, R. P. Concentration profile for a polymer-polymer interface. 1. Identical chemical composition and molecular weight. *Macromolecules* **1989**, *22*, 3018−3021. (b) Agrawal, G.; Wool, R. P.; Dozier, W. D.; Felcher, C. P.; Zhou, J.; Pispas, S.; Mays, J. W.; Russel, T. P. Interdiffusion of polymers across interfaces. *J. Polym. Sci., Polym. Phys.* **1996**, *34*, 2919−2940.
(47) Wool, R. P. *Polymer Interfaces. Structure and Strength*; Carl Hanser Verlag: Munich, 1995.
(48) McCrum, N. G.; Read, B. E.; Williams, G. *Anelastic and Dielectric Effect in Polymeric Solids*; John Wiley & Sons: New York, 1967.
(49) Tomba, J. P.; Carella, J. M.; Pardo, E.; Lopez, S.; Pastor, J. M. A generalized method to calculate diffusion rates in polydispersed systems. Further results on Rouse dynamics in the concentrated regime. *Macromol. Rapid Commun.* **2000**, *21*, 983−989.